PLANT SCIENCES

The plant cuticle regulates apoplastic transport of salicylic acid during systemic acquired resistance

Gah-Hyun Lim¹*, Huazhen Liu¹, Keshun Yu¹, Ruiying Liu¹, M. B. Shine¹, Jessica Fernandez², Tessa Burch-Smith², Justin K. Mobley³, Nicholas McLetchie⁴, Aardra Kachroo¹, Pradeep Kachroo^{1†}

The plant cuticle is often considered a passive barrier from the environment. We show that the cuticle regulates active transport of the defense hormone salicylic acid (SA). SA, an important regulator of systemic acquired resistance (SAR), is preferentially transported from pathogen-infected to uninfected parts via the apoplast. Apoplastic accumulation of SA, which precedes its accumulation in the cytosol, is driven by the pH gradient and deprotonation of SA. In cuticle-defective mutants, increased transpiration and reduced water potential preferentially routes SA to cuticle wax rather than to the apoplast. This results in defective long-distance transport of SA, which in turn impairs distal accumulation of the SAR-inducer pipecolic acid. High humidity reduces transpiration to restore systemic SA transport and, thereby, SAR in cuticle-defective mutants. Together, our results demonstrate that long-distance mobility of SA is essential for SAR and that partitioning of SA between the symplast and cuticle is regulated by transpiration.

Copyright © 2020
The Authors, some rights reserved; exclusive licensee American Association for the Advancement of Science. No claim to original U.S. Government Works. Distributed under a Creative Commons Attribution NonCommercial License 4.0 (CC BY-NC).

INTRODUCTION

The plant cuticle is a hydrophobic layer that covers the aerial surface of plants and forms the first line of contact with the environment. The mature cuticle is composed of cutin and cuticular wax. The cuticular wax is a complex mixture of very-long-chain fatty acid (VLCFA) derivatives formed upon elongation of fatty acids (FAs), which are biosynthesized in the plastids [reviewed in (1, 2)]. FA biosynthesis is catalyzed by a multienzyme complex comprising β-ketoacylacyl carrier protein (ACP) synthase (KAS), β-ketoacyl-ACP reductase, β-hydroxyacyl-ACP dehydrase, and enoyl-ACP reductase. These enzymes catalyze successive addition of two-carbon (C) units on an FA precursor, which is conjugated to the ACP backbone. The C16 and C18 FAs are important precursors of cuticular wax synthesis and are extended to form VLCFAs (C > 20). The C16 and C18 FAs are also required for biosynthesis of cutin, a polymer of C16 and C18 diacids and ω- and midchain hydroxy FAs. Because of the importance of C16 and C18 FA levels in both wax and cutin biosynthesis, reductions in the flux of these FA s impair cuticle development. This is evident in the Arabidopsis acp4 mutant, which contains reduced FA levels and, as a result, has ruptured cuticle (3).

Besides serving as a physical barrier against the environment, the cuticle is known to be important for the broad-spectrum defense signaling mechanism, systemic acquired resistance (SAR) (3–5). SAR is a form of systemic immunity that protects distal uninfected parts of the plant against secondary infections. SAR involves the generation of a mobile signal in the primary infected leaves, which when translocated to distal uninfected portions, activates defense responses, resulting in systemic disease resistance (6–8). A number of chemical SAR inducers have been identified including salicylic acid (SA) (9), which accumulates in both inoculated and uninoculated leaves

and is essential for SAR (9). It is generally assumed that despite the fact that SA biosynthesis in the distal tissue is absolutely essential for SAR, SA is not a translocated mobile signal during SAR (10). This assumption was derived from a study that analyzed grafts between wild-type and bacterial salicylate hydroxylase (nahG)–expressing tobacco plants. That study found that wild-type scions grafted to nahG rootstocks were SAR competent in response to primary infection in the nahG rootstocks, whereas nahG scions grafted to wild-type rootstocks were compromised for SAR. Notably, the distal SA levels in these plants only differed by ~10 ng/g fresh weight (FW) (10), which is well within variations seen in basal SA levels (10 to 100 ng/g FW).

Recent analysis has shown that translocation of SA from primary infected tissue to the distal tissue likely occurs via apoplast (space between cell wall and plasma membrane) (11); pathogen infection results in increased SA accumulation in the apoplastic compartment, and this accumulation is unaffected by defects in symplastic transport via plasmodesmata (PD) (11). In contrast, two other SAR-associated chemical signals, glycerol-3-phosphate (G3P) and azelaic acid (AzA), are transported preferentially via PD, and defects in PD permeability interfere with their transport from infected to distal tissues (11). AzA functions upstream of G3P and the AzA-G3P branch functions in parallel to SA-derived signaling during SAR (11–15). A fourth SAR inducer, pipecolic acid (Pip), functions upstream of the AzA-G3P branch to confer SAR by inducing the biosynthesis of free radicals (14, 16–18). Pip is converted to N-hydroxy Pip (NHP) via flavin monooxygense-catalyzed reaction (19, 20). Relationship between NHP and other SAR signals remains unclear at present (21). Notably, transport of both SA and G3P is essential for Pip accumulation in the distal tissues (16). Thus, coordinated transport and feedback regulation among the various chemical signals eventually activates SAR in plants.

This study was undertaken to uncover the factors that regulate SA transport from local to distal tissues and to determine the biological consequences of impaired SA transport during SAR. We show that transport of SA from local to distal tissues is indeed essential for SAR, and this transport is governed by water potential in the infected tissue. We also find that SA is partitioned between symplast,

¹Department of Plant Pathology, University of Kentucky, Lexington, KY 40546, USA. ²Department of Biochemistry & Cellular and Molecular Biology, University of Tennessee, TN 37996, USA. ³Department of Chemistry, University of Kentucky, Lexington, KY 40506, USA. ⁴Department of Biology, University of Kentucky, Lexington, KY 40506, USA.

^{*}Present address: Advanced Radiation Technology Institute, Korea Atomic Energy Research Institute, Jeongeup 56212, Korea.

[†]Corresponding author. Email: pk62@uky.edu

apoplast, and cuticular waxes, and transport of SA into waxes might regulate stomatal closing in response to pathogen infection.

RESULTS

ACP4 and MOD1 are required for apoplastic transport of SA

Earlier, we showed that mutations in ACP4 impaired SAR (3). To determine the underlying cause, we first evaluated SA and G3P levels in these plants, because these chemicals regulate the two parallel branches of SAR pathway. The acp4 plants accumulate wild-typelike levels of SA, SA glucoside (SAG), and G3P in infected leaves (Fig. 1, A and B), suggesting that their SAR defect is not due to impaired SA or G3P biosynthesis in response to pathogen infection. We next monitored transport of SA and G3P, because distal transport of both is essential for the induction of SAR (16). The acp4 plants accumulated wild-type-like G3P levels in the petiole exudates (PEX) of both mock- and Pseudomonas syringae pv tomato (Pst) avrRpt2infected leaves (Fig. 1C). This was consistent with the normal PD permeability of acp4 plants (Fig. 1D), which is the preferred route for G3P transport (11). For PD permeability, plants were bombarded with a green fluorescent protein (GFP)-expressing vector using microprojectiles, and layers of cells containing trafficked GFP surrounding the transformed cells were counted. Unexpectedly, unlike G3P transport, the *acp4* mutant was defective in SA transport based on the significantly reduced SA levels in their PEX after *Pst avrRpt2* infection (Fig. 1E). Consistent with phloem loading of SA via the apoplast, pathogen-infected acp4 plants also accumulated reduced SA in their apoplast (fig. S1A). To determine if the impaired SA transport was associated with reduced FA flux in acp4 plants, we examined SA transport in *mod1*, another mutant defective in FA flux. In addition, we also examined SA transport in fad2, fad6, and fad7 fad8 mutants, which contain reduced FA levels in membrane lipids. The mod1 mutant is defective in the key FA biosynthetic enzyme enoyl-ACP reductase (fig. S1B) (22) and has reduced levels of multiple FA species and total lipids (fig. S1, C and D). Despite the essential function of enoyl-ACP reductase in FA biosynthesis, mod1 plants are viable due to the leaky nature of the mutation (22). Like acp4, mod1 plants were also impaired in SA transport into PEX (Fig. 1E) and apoplast (fig. S1A), despite wild-type-like SA levels in infected leaves (Fig. 1A). In contrast, PEX from all fad mutants contained wildtype-like levels of SA (fig. S1E), suggesting that the reduction in membrane FA species of acp4 and mod1 plants is unlikely to be responsible for their impaired SA transport into PEX. Both acp4 and mod1 plants contained wild-type-like levels of benzoic acid (BA) (fig. S1F), an aromatic carboxylic acid that is structurally similar to SA and is thought to serve as a SA precursor (fig. S1G). Notably, unlike SA, BA levels did not increase after pathogen infection, which is consistent with the fact that most of the SA in Arabidopsis is derived from isochorismate synthase (ICS; fig. S1G) catalyzed reaction (23).

Like acp4, mod1 plants also contained wild type–like levels of G3P in their infected leaves, showed wild-type–like PD permeability, and were competent for G3P transport into PEX (Fig. 1, B and D). These results suggested that acp4 and mod1 plants were impaired in SA transport. To confirm this, we examined the transport of 14 C-SA in these plants. The procedure involved infiltration of SA into the apoplastic space, which presumably could passively move to the distal tissue (24). Therefore, we first determined the minimal SA concentration that could be infiltrated without increasing PEX-SA levels. PEX was collected from Col-0 leaves infiltrated with 20, 100, or 500 μ M

SA followed by SA quantification. Infiltration of 100 and 500 μM SA resulted in SA accumulation in the PEX, whereas 20 µM SA did not (fig. S1H). We then coinfiltrated 10 mM MgCl₂ + 20 μ M ¹⁴C-SA (mock) or Pst avrRpt2 + 20 μM ¹⁴C-SA in wild-type and acp4 mutant plants and quantified the amount of ¹⁴C-SA in their infiltrated and distal (untreated) leaves 48 hours later. Coinfiltration of 14C-SA with Pst avrRpt2 infection of increased 14C levels in the distal leaves of wild-type plants by ~2.5-fold (Fig. 1F). In comparison, mod1 and acp4 plants did not show a similar increase (Fig. 1F and fig. S1I). Thin layer chromatographic analysis of extracts from infected and distal leaves detected a band corresponding to the SA standard (Fig. 1G), which was confirmed as SA by mass spectrometric (MS) analysis of the eluted product (fig. S1J). This suggested that SA was not modified during transport and is consistent with MS-based analysis of PEX-SA (Fig. 1E). Together, these results suggested that ACP4 and MOD1 are required for apoplastic transport of SA into the distal tissue.

The mod1 plants are impaired in cuticle formation

The FA defect in acp4 plants results in defective cuticle formation (fig. S1B) (3). Like acp4 (3), mod1 plants also show reduced growth and altered morphology (Fig. 2A and fig. S2A). We tested if mod1 plants also had defects in the cuticle by staining Col-0 and mod1 leaves with toluidine blue, a hydrophilic dye that does not penetrate intact cuticle (25). Toluidine blue rapidly penetrated *mod1* leaves on both the adaxial and abaxial sides, suggesting cuticular permeability (Fig. 2B and fig. S2B). This was further supported by the rapid leaching of chlorophyll from *mod1* leaves (fig. S2C). Transmission electron microscopy of leaf epidermal cells showed that the cuticle of the *mod1* mutant was diffuse and electron opaque versus the continuous and electrondense osmiophilic layer outside the cell wall of wild-type leaves (Fig. 2C, marked by an arrow). Scanning electron micrographs of leaf surfaces showed stretched and highly folded epidermis in *mod1* (Fig. 2D). To determine if this defect in cuticle structure was associated with alterations in the content and/or composition of cuticular waxes or cutin polyester monomers, we compared the levels of waxes and cutin monomers in wild-type and mod1 leaves. The mod1 leaves showed elevated levels of 26- and 28-carbon primary alcohols compared with wild-type plants (fig. S2D) but contained wild-type-like levels of cutin monomers (fig. S2E). Increased accumulation of cuticular components is often observed in cuticle mutants and thought to play a compensatory role contributing to the survival of these mutants (5, 26). Together, these results show that, like ACP4, MOD1 is important for cuticle development.

Impaired transport of SA compromises SAR

Earlier, we showed that cuticle defects were associated with compromised SAR (3–5). This was also true for *mod1* plants, which were compromised in SAR (Fig. 3A). We considered the possibility that the cuticle defect in *acp4* and *mod1* plants might be linked to their inability to transport SA during SAR. To test this, we first evaluated the SAR phenotype and SA transport in the cuticle defective *lacs2* mutant (27, 28). LACS2 catalyzes a downstream step in the cuticle biosynthesis (fig. S1B). Like *mod1*, the *lacs2* plants showed compromised SAR (Fig. 3A) and accumulated significantly lower levels of SA in PEX as compared with wild-type plants (Fig. 3B). As an additional test, we evaluated SA transport in wild-type leaves after mechanical abrasion of the cuticle followed by pathogen infection; wild-type leaves were gently rubbed with a buffered solution containing celite and bentonite (3) followed by *Pst avrRpt2* infection 12 hours after

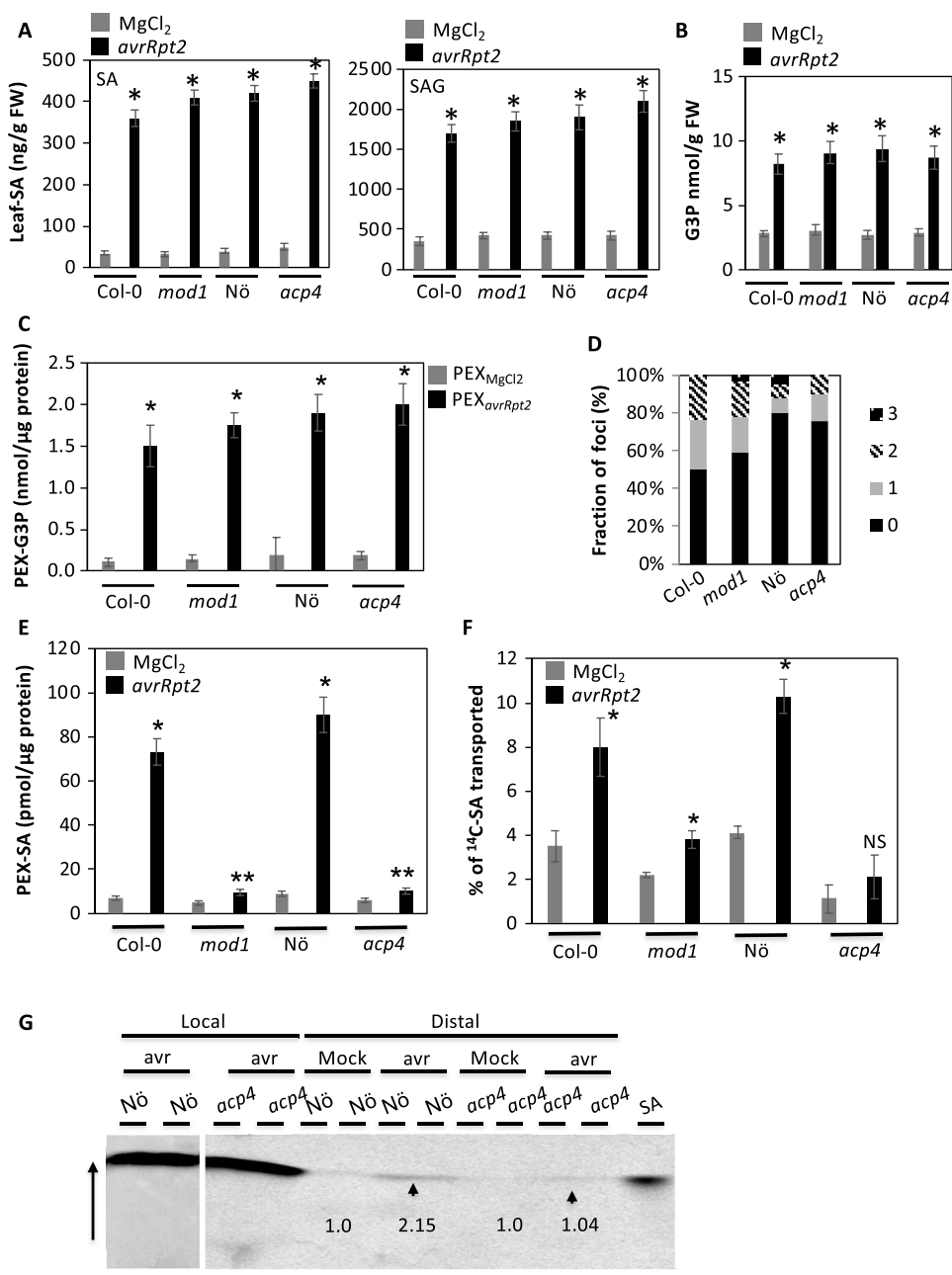
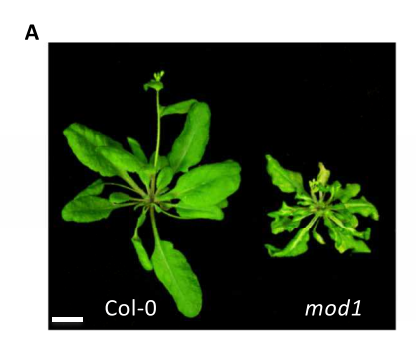
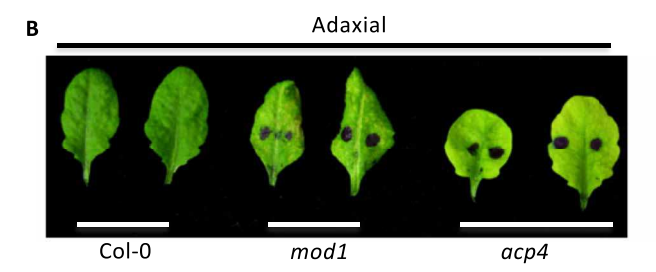
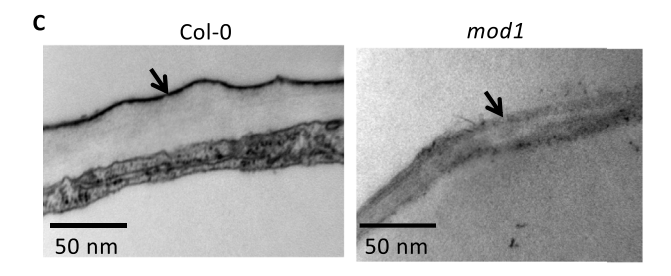


Fig. 1. ACP4 and MOD1 are required for distal transport of SA. (A) SA and SAG levels in local tissues after mock (10 mM MqCl₂) and pathogen (avrRpt2) inoculations. The leaves were sampled 48 hours after treatments, and the experiment was repeated two times with similar results. Asterisks denote a significant difference with respective mock-inoculated samples (t test, P < 0.0001). Columbia (Col-0) and Nössen (Nö) are wild-type ecotypes for mod1 and acp4, respectively. (B) G3P levels in local tissues after mock and pathogen (avrRpt2) inoculations. The leaves were sampled 24 hours after treatments, and the experiment was repeated two times with similar results. Asterisks denote a significant difference with respective mock-inoculated samples (t test, P < 0.0005). (C) G3P levels in PEX collected from mock (PEX_{MaCI2}) – and avrRpt2 (PEX_{avrRot2})-inoculated plants. The experiment was repeated three times with similar results. Asterisks denote a significant difference with respective mock-inoculated samples (t test, P < 0.0007). (D) Size of foci measured as numbers of rings of cells containing P30-2XGFP punctae around a transformed cell 48 hours after treatment in wild-type (Col-0 or Nö) or acp4 and mod1 leaves. (E) SA levels in PEX collected from mock (PEX_{MqCl2}) – and avrRpt2 (PEX_{avrRpt2})–inoculated plants. Results are representative of four independent experiments. Single (t test, P < 0.0001) and double (t test, P < 0.004) asterisks denote a significant difference with respective mock-inoculated samples or between indicated pairs, respectively. (F) Quantification of radioactivity transported to distal tissues of mock- and avrRpt2-inoculated plants. Leaves were infiltrated with 20 μM solution of ¹⁴C-SA and sampled 48 hours after mock (MgCl₂) or avrRpt2 inoculations. The error bars indicate SD. Asterisks denote a significant difference with respective mock-inoculated samples (t test, P < 0.006). NS indicates data not significantly different. (G) Autoradiograph of TLC plate showing transport of ¹⁴C-SA from the local to distal leaves. 14C-SA (20 µM) was mixed with MgCl₂ (mock) or avrRpt2 and infiltrated into the local leaves of wild type (Nö) and acp4. Both local and distal leaves were sampled 48 hours after treatment and analyzed on a silica TLC plate using toluene/methanol/acetic acid (45:8:4, by volume) solvent system. Arrowhead indicates position of the ¹⁴C-SA. Vertical arrow indicates direction of the run. Numbers below the bands indicate relative intensity of bands in mock versus avr samples quantified using ImageQuant TL image analysis software.







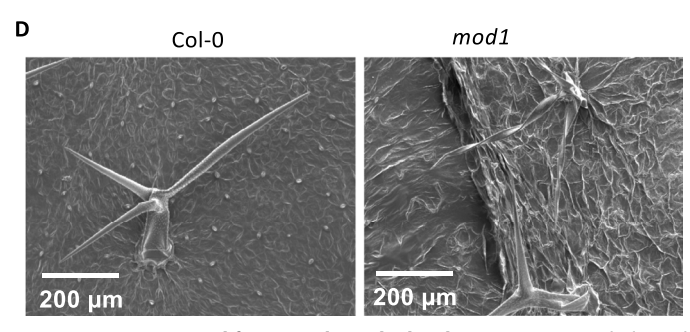


Fig. 2. *MOD1* is required for normal cuticle development. (**A**) Morphological phenotype of 4-week-old Col-0 and *mod1* plants (scale, 0.5 cm). Photo credit: P.K., University of Kentucky. (**B**) Toluidine blue–stained leaves from 4-week-old leaves of Col-0, *mod1*, and *acp4* plants. The leaves were stained on their adaxial surface for 5 min. Photo credit: P.K., University of Kentucky. (**C**) Transmission electron micrographs showing cuticle layer on adaxial surface of Col-0 and *mod1* plants. Arrows indicate cuticle, which is electron dense in Col-0 leaves. Scale bars, 50 nm. (**D**) Scanning electron micrographs showing abaxial surface of Col-0 or *mod1* leaves. Scale bars, 200 μm.

abrasion. SA levels in PEX from mechanically abraded leaves were significantly lower than those in PEX from intact leaves (Fig. 3C). Mechanical abrasion did not induce jasmonic acid (JA)— or abscisic acid (ABA)—responsive genes at 12 hours after treatment (fig. S3A), suggesting that reduced PEX-SA levels in these plants were not due to antagonism between SA and JA or ABA. Moreover, Pst inoculation itself induces JA and ABA in wild-type plant and that does not inhibit SA transport or SAR (29, 30). A reduction in PEX-SA was

consistent with the result that leaf abrasion before Pst avrRpt2 inoculation compromised SAR in wild-type plants (Fig. 3D). Together, these results suggested that an intact cuticle might be important for the proper transport of SA into distal tissue, and this in turn might be necessary for the onset of SAR. To test this further, we assayed SA-mediated SAR in acp4, mod1, and lacs2 plants. Localized application of SA conferred SAR in wild-type plants but not in acp4, mod1, or lacs2 plants (Fig. 3E and fig. S3B). Next, we assayed Pip levels in local and distal tissues, since SA transport is required for de novo biosynthesis of Pip in distal leaves (16). The acp4 and mod1 plants accumulated wild-type-like levels of Pip in infected leaves but contained significantly reduced levels of Pip in their distal leaves (Fig. 3, F and G). As expected, Pip, G3P, and AzA, which function in the second branch of SAR signaling and cannot confer SAR in SA-deficient plants (14, 16), were unable to induce SAR in acp4 and mod1 (Fig. 3, H and I). Together, these results strongly indicate that transport of SA is essential for SAR.

Our results supporting the mobility of SA during SAR are contrary to a previous report that concluded that SA was not a mobile SAR signal but was required for SAR induction in the distal tissues (10). That study presumed a lack of distal SA transport in the SAdeficient nahG transgenic plants (express the SA-catabolizing nahG). To test this presumption, we assayed SA levels in PEX collected from pathogen-infected nahG plants. Pst avrRpt2-infected Arabidopsis (Dijon; Di-3 ecotype) and tobacco mosaic virus (TMV)-infected tobacco plants were used. Pathogen infection did induce SA accumulation in the PEX of nahG plants (Arabidopsis and tobacco), albeit at significantly lower levels than in wild-type plants (Fig. 4A). Notably, the relative increase in SA levels (pathogen-responsive versus basal levels) was higher in nahG plants than in wild-type plants (fig. S3C). We then analyzed the transport of ¹⁴C-SA in wild-type and nahG Arabidopsis plants. Leaves of wild-type Di-3 or nahG transgenic plants were coinfiltrated with 20 µM ¹⁴C-SA + 10 mM MgCl₂ (mock) or 20 μ M 14 C-SA + *Pst avrRpt2* (10 5 cfu in 10 mM MgCl₂). Amount of ¹⁴C in infected and distal leaves was quantified 48 hours later. Consistent with the nahG-derived catabolism of SA (31), nahG plants contained significantly less ¹⁴C-SA than wild-type plants in their infiltrated leaves (fig. S3D). Yet, the relative (infiltrated versus systemic) percentage of ¹⁴C in the distal leaves of nahG plants was comparable to that in wild-type plants; nearly 5% of ¹⁴C levels in infiltrated leaves were detected in distal leaves of nahG plants versus ~3% in wild-type plants (Fig. 4, B and C). In contrast, sid2 plants (mutation in ICS; fig. S1G), which are impaired in SA biosynthesis (23), did not show any SA accumulation in PEX (fig. S3E). Together, these results suggested that nahG plants are competent in SA transport. As additional bioassays to reconfirm transport of SA in nahG plants, we first quantified Pip levels in inoculated and distal tissue of wild-type and nahG plants because Pip accumulation in distal tissues is dependent on SA (16, 18). Both Arabidopsis (Fig. 4D) and tobacco (Fig. 4E) nahG plants accumulated wild-type-like levels of Pip in the inoculated leaves. Notably, although nahG plants showed statistically significant induction of Pip in distal tissue, these levels were lower than in wild-type plants (Fig. 4, D and E). Unlike nahG, sid2 plants showed significantly reduced levels of Pip in their distal leaves (16, 18). The reduced Pip accumulation in distal tissue of nahG plants could be due to their inability to maintain threshold SA levels and, thereby, initiate the SA-Pip feedback loop (16). As an additional test, we generated reciprocal grafts between wild-type and nahG tobacco plants and monitored accumulation of the SA marker protein PR-1 in

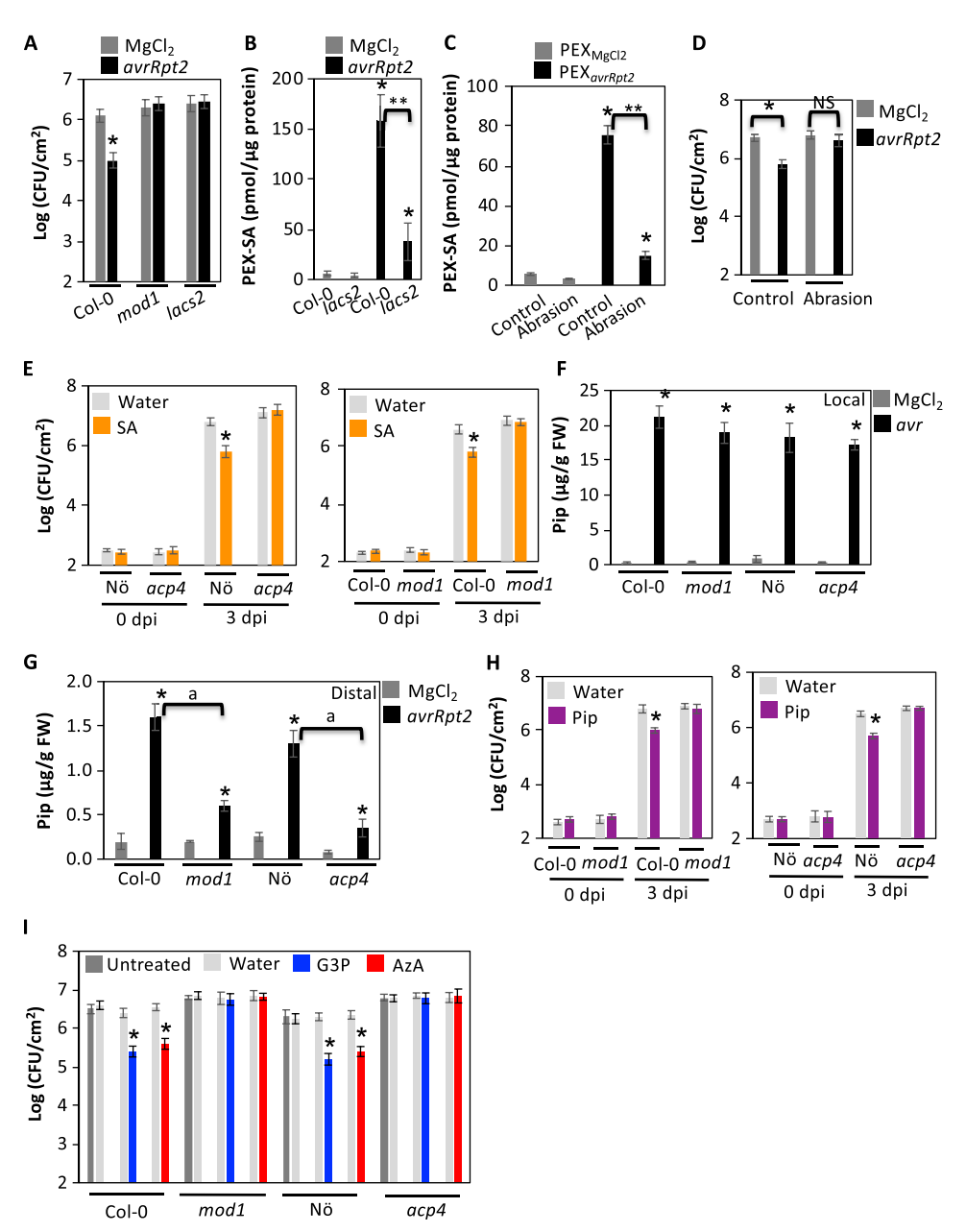


Fig. 3. Exogenous application of SA, G3P, or Pip is unable to confer SAR on mod1 or acp4 plants. (A) SAR response in distal leaves of Col-0, mod1, and lacs2 plants treated locally with MgCl₂ or avrRpt2. The virulent pathogen (DC3000) was inoculated 48 hours after local treatments. CFU indicates colony forming units. Asterisks denote a significant difference with respective mock-inoculated samples (t test, P < 0.0001). (B) SA levels in PEX collected from mock (PEX_{MoCl2}) – and avrRpt2 (PEX_{avrRpt2}) – inoculated Col-0 and lacs2 plants. Single and double asterisks denote a significant difference with respective mock-inoculated samples (t test, P < 0.0001) or indicated pair (t test, P < 0.0001), respectively. (C) SA levels in PEX collected from mock (PEX_{MQCI2}) – and avrRpt2 (PEX_{avrRpt2}) – inoculated plants. The local leaves were abraded to damage the cuticle 12 hours before inoculation. Results are representative of two independent experiments. Single and double asterisks denote a significant difference with respective mock-inoculated samples (t test, P < 0.0006) or indicated pair (t test, P < 0.0001), respectively. (**D**) SAR response in distal leaves of untreated or cuticle abraded plants shown in (C). The virulent pathogen (DC3000) was inoculated 48 hours after mock or avr inoculations. Asterisks denote a significant difference with respective mock-inoculated samples (t test, P < 0.0001). NS indicates "not significant." (E) SAR response in distal leaves of wild-type (Col-0 or Nö), acp4, or mod1 plants treated locally with water or SA (500 µM). The virulent pathogen (DC3000) was inoculated 48 hours after local treatments. Error bars indicate SD (n = 4). Asterisks denote a significant difference with mock (t test, P < 0.0002). The experiment was repeated three times with similar results. (F and G) Pip levels in local (F) and distal (G) tissues of wild-type (Col-0 or Nö), acp4, or mod1 plants after mock and avrRpt2 inoculations. The leaves were sampled 48 hours after treatments. Asterisks denote a significant difference with mock (t test, P < 0.0001). "a" denotes significant difference between avrRpt2-inoculated wild type and mutants (P < 0.0005). The experiment was repeated three times with similar results. (H) SAR response in distal leaves of wild-type (Col-0 or Nö), acp4, or mod1 plants treated locally with water or Pip (1000 μM). The virulent pathogen (DC3000) was inoculated 48 hours after local treatments. Asterisks denote a significant difference with mock (t test, P < 0.0001). The experiment was repeated two times with similar results. (I) SAR response in distal leaves of wild-type (Col-0 or Nö), acp4, or mod1 plants treated locally with water, G3P (100 μM), or AzA (1000 μM). The virulent pathogen (DC3000) was inoculated 48 hours after local treatments. Asterisks denote a significant difference with mock (t test, P < 0.0005). The experiment was repeated three times with similar results.

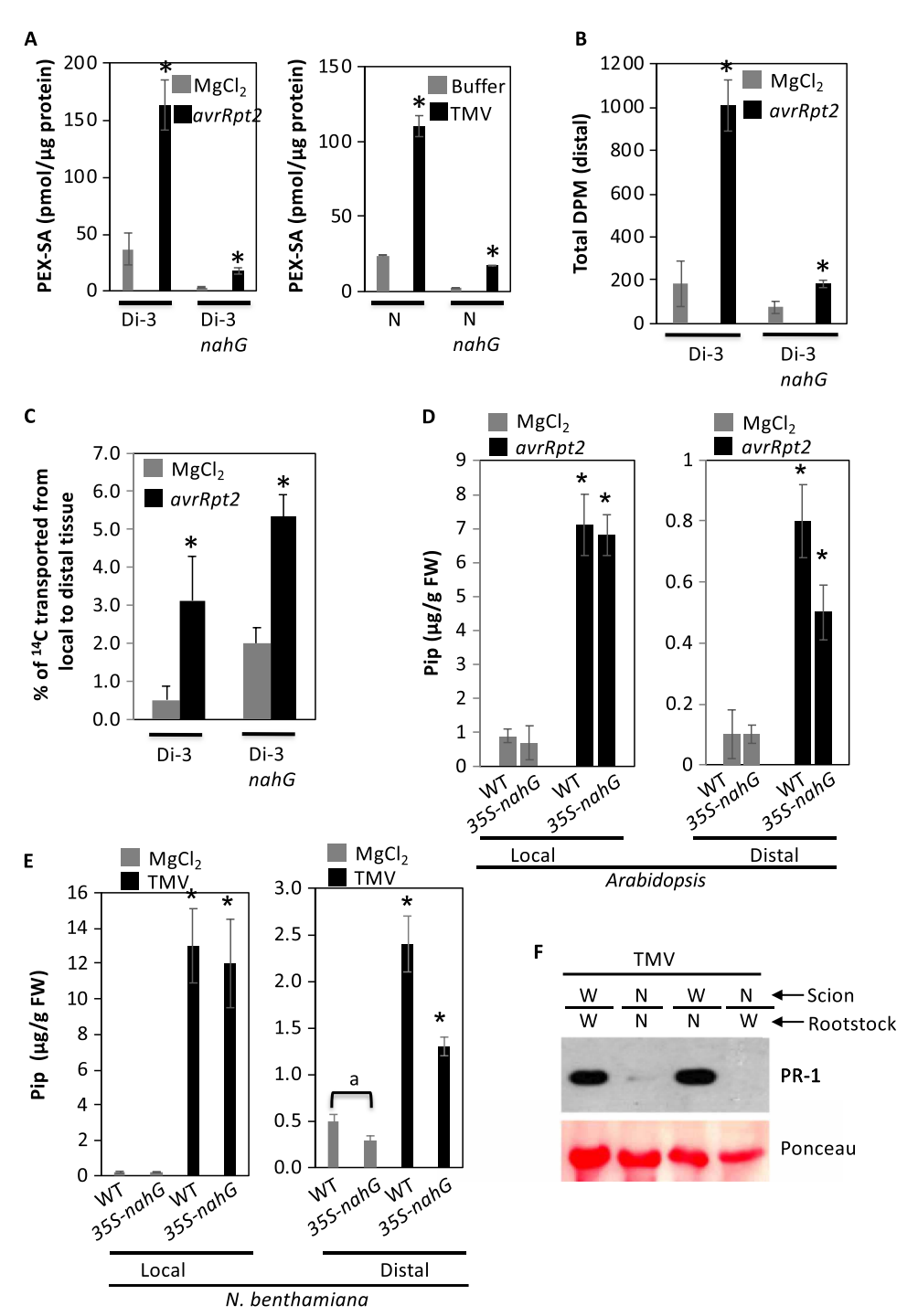


Fig. 4. NahG plants are competent in SA transport. (**A**) SA levels in PEX collected from mock (PEX_{MgCI2})– or pathogen (*avrRpt2* or TMV)–infected *Arabidopsis* (Di-3) or tobacco (Samsung N background) wild-type and *nahG* plants. Results are representative of three independent experiments. Asterisks denote significant differences from respective mock-inoculated samples (t test, P < 0.001). (**B**) Levels of ¹⁴C-SA in distal tissue of *Arabidopsis* wild-type (Di-3 ecotype) or Di-3 nahG plants. *Arabidopsis* leaves were coinfiltrated with 20 μM ¹⁴C-SA and MgCl₂ or *Pst avrRpt2*. Forty-eight hours later, amount of radiolabel in SA extracts from the leaves was quantified. Results are representative of three independent experiments. Asterisks denote significant differences (t test, P < 0.004). (**C**) Percentage of ¹⁴C-SA transported from local to distal tissue of Di-3 and Di-3 nahG plants shown in (B). Asterisks denote significant differences (t test, P < 0.002). (**D** and **E**) Pip levels in local and distal tissue of *Arabidopsis* (D) or tobacco (E) plants after mock and pathogen inoculations. The *Arabidopsis* and tobacco distal leaves were sampled 48 or 140 hours after inoculation, respectively. Asterisks denote significant differences from mock (t test, P < 0.0001). The experiment was repeated three times with similar results. (**F**) Protein immunoblot showing PR-1 levels in the scion (distal) of tobacco grafts that were inoculated with TMV in the rootstock (local). W and N indicate wild type and nahG. Scion leaf samples were collected 5 days after TMV inoculation. Ponceau-S staining of the immunoblot was used as the loading control. The experiment was repeated twice with similar results.

scion leaves (distal tissue) in response to TMV infection in the rootstock (local). As expected, PR-1 accumulated in scions of wild-type $_{\rm rootstock}$ X wild-type $_{\rm scion}$ grafts but not in nahG $_{\rm rootstock}$ X nahG $_{\rm scion}$ grafts (Fig. 4F). Notably, TMV infection of rootstocks also induced PR-1 accumulation in the scion of nahG $_{\rm rootstock}$ X wild-type $_{\rm scion}$, but not wild-type $_{\rm rootstock}$ X nahG $_{\rm scion}$ grafts (Fig. 4F). Together, these results suggest that nahG plants transport enough SA to induce PR-1 accumulation in the distal leaves. However, at present, we are unable to rule out an alternate possibility that a portion of SA in wild-type $_{\rm scion}$ is synthesized de novo.

Next, we determined whether the impaired SA transport in *acp4* and *mod1* plants affected their ability to generate or perceive the SAR signal. For this, we collected PEX from MgCl₂ (PEX_{MgCl2}) or *Pst avrRpt2* (PEX_{avr}) preinfiltrated wild-type (PEX-Col-0 or PEX-Nö), *mod1* (PEX-*mod1*), and *acp4* (PEX-*acp4*) plants. These PEX were then infiltrated into a fresh set of wild-type, *mod1*, or *acp4* plants followed by infection of distal leaves with *Pst* DC3000 (fig. S4). The growth of *Pst* DC3000 was monitored at 0 and 3 days post inoculation (dpi). The PEX_{avr} from either Col-0 or *mod1* conferred SAR on Col-0 plants, but not on *mod1* plants (fig. S4A). Similarly, the PEX_{avr} from *acp4* plants induced SAR on Nö, but not *acp4* plants (fig. S4B). These re-

sults suggest that PEX from *acp4* and *mod1* confers SAR on wild-type plants because they contain the unidentified mobile signal. However, PEX from wild-type plants is unable to confer SAR on *mod1* and *acp4* plants, likely because transport of both unidentified mobile signal and SA is essential for SAR.

Cuticle impairment reduces water potential and, thereby, apoplastic transport of SA

The cuticle is an important physical barrier that prevents water loss from leaves. We considered the possibility that increased transpiration in cuticle-defective mutants might alter the distal transport of SA by reducing osmotic pressure. To test this, we assayed SA transport in Nö and *acp4* plants grown under high humidity. This is because high humidity has been shown to reduce transpiration without activating ABA-derived signaling (32, 33), which negatively regulates SA level and SAR (34). Humidity was increased by covering plants with a transparent dome or by placing them in a growth chamber maintained at high humidity (90% relative humidity). SA levels were quantified in PEX collected from mock- and pathogen-infected plants. The PEX-SA levels of pathogen-infected dome-covered plants were higher than in the uncovered plants (Fig. 5A). Furthermore,

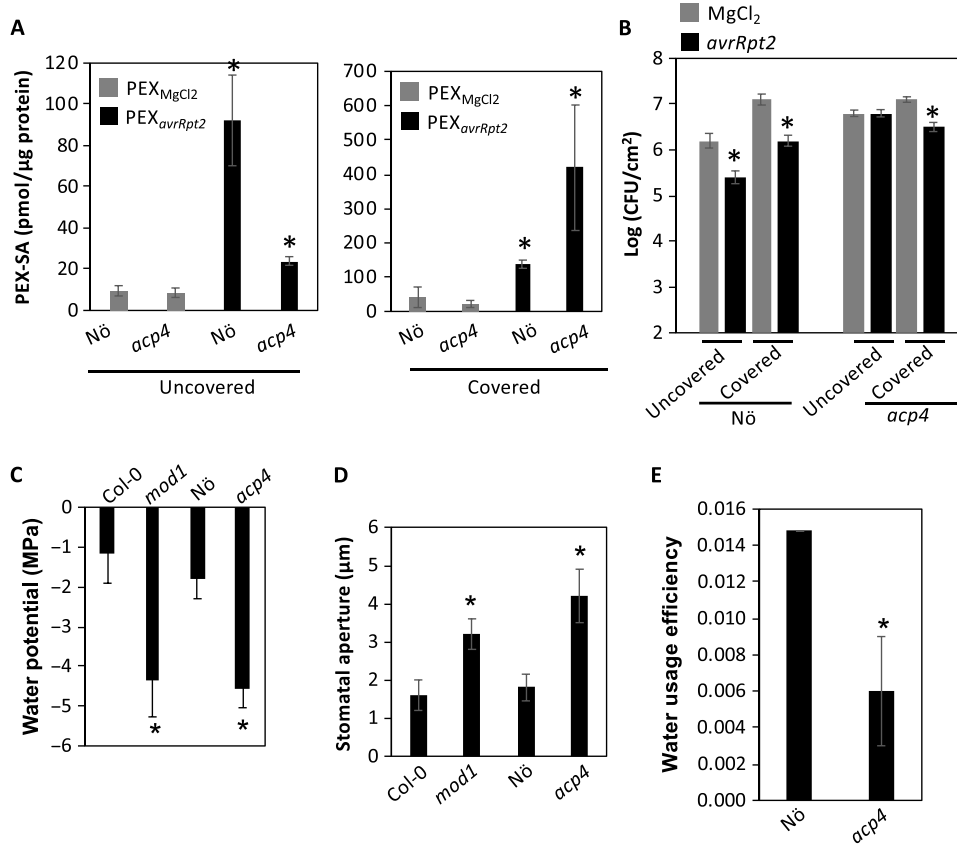


Fig. 5. Distal transport of SA is associated with water potential. (A) SA levels in PEX collected from mock (PEX_{MgCl2})— and avrRpt2 (PEX_{avrRpt2})—inoculated Nö and acp4 plants. A week before inoculations, one set of plants was covered with a transparent dome to increase humidity and reduce transpiration. Results are representative of three independent experiments. Asterisks denote a significant difference with respective mock-inoculated samples (t test, P < 0.001). (B) SAR response in distal leaves of Nö and acp4 that were grown in open or covered with a transparent dome. The virulent pathogen (DC3000) was inoculated 48 hours after local treatments. Error bars indicate SD (n = 4). Asterisks denote a significant difference with mock (t test, P < 0.0001). The experiment was repeated two times with similar results. (C) Leaf water potential of indicated genotypes. Values are means \pm SD (n = 15). Asterisks denote a significant difference with mock (t test, t test, t values are means t values are

covered acp4 plants accumulated wild-type-like or higher SA in PEX after pathogen infection. Consistent with this result, the covered acp4 plants were SAR competent (Fig. 5B), even though the increased humidity in covered plants resulted in enhanced local susceptibility in both Nö and acp4 plants (Fig. 5B)(35). Similar results were obtained when plants were grown in a humidifying chamber (fig. S4C). These results suggested that the distal movement of SA was driven by water transpiration; increased water loss in the cuticle-defective acp4 and mod1 plants inhibited the distal transport of SA in these plants. Consistent with this notion, both acp4 and mod1 plants showed low water potential (Fig. 5C) and increased transpiration, which was associated with open stomata (Fig. 5D). The water usage efficiency (WUE) of acp4 plants was monitored by measuring gas exchange because the defective cuticle and open stomata phenotypes were likely to have an additive effect on overall transpiration rates and, thereby, WUE. As expected, the acp4 plants showed reduced WUE (Fig. 5E). Together, these results suggest that increased cuticle permeability leads to reduced water potential and WUE, which in turn was associated with impaired apoplastic transport of SA.

SA exists in its deprotonated form at cytosolic pH and is channeled into cuticle

The pKa of COOH and phenol groups of SA are 2.98 and 13.6, respectively (36). Therefore, the COOH group of SA is expected to predominantly exist in its deprotonated form (COO⁻) at the neutral to slight alkaline pH (~7 to 7.5) of the cytosol and acidic pH (~4.5) of the apoplast (37). Nuclear magnetic resonance (NMR) analyses of pH-dependent chemical shifts in ¹H showed that the COOH group of SA does indeed exist in its deprotonated form at pH 7.0 and 4.5 but remains protonated at more acidic pH (2.5; Fig. 6A). This suggests that cellular SA exists primarily as deprotonated species. We tested the membrane permeability of deprotonated SA by assaying the uptake of ¹⁴C-SA by protoplasts. Arabidopsis protoplasts incubated with ¹⁴C-SA showed ~22% uptake of ¹⁴C within 1 hour at pH 5.7 (Fig. 6B). Notably, SA transport was significantly higher (~45%) at pH 4.5 (Fig. 6B). In contrast, protoplasts that were allowed to regenerate their cell walls and accumulate callose for 24 hours before incubation with ¹⁴C-SA did not show uptake of ¹⁴C at either pH. This suggested that deprotonated SA was membrane permeable and that this permeability was influenced by the cellular pH. Thus, uptake of apoplastic SA in the distal tissue would be greatly facilitated by the acidic pH of the apoplast. This further suggested that transport of SA across the plasma membrane might involve a proton pump. We tested the possibility by assaying SA transport in the presence of sodium orthovanadate and omeprazole, which are well-known inhibitors of proton pumps (38, 39). Both chemicals did inhibit SA transport in a concentrationdependent manner (Fig. 6B, bottom), strongly supporting the possible involvement of proton pump(s) in SA transport. In contrast to protoplasts, ¹⁴C-SA was not taken up by intact chloroplasts at pH 7.5 (Fig. 6B). We were unable to conduct uptake experiments at pH 4.5 since chloroplasts lysed at this pH. These results suggest that cytosolic SA is not transported into chloroplasts.

We considered the possibility that preferential distribution of SA to the cuticle in the *acp4* and *mod1* mutants may be responsible for their reduced apoplastic SA. This assumption was supported by the plasma membrane permeability of deprotonated SA, the normal levels of total SA in these mutants, and the fact that higher transpiration resulting from their cuticle defect would be expected to increase water flow toward the exterior. To test this, we assayed SA levels in

cuticle wax extracted from pathogen-infected leaves of wild-type and mutant plants. The absence of membrane lipids in the cuticle wax fraction (fig. S5A) increased confidence that our extraction procedure did not release cytosolic SA into the wax fraction. Wax fractions also did not contain detectable levels of Pip. Both spray and leaf infiltration of Pst avrRpt2 increased the SA content in cuticle wax by ~4.5- to 6-fold (Fig. 6C). Infection with the virulent fungal pathogen Colletotrichum higginsianum or avirulent turnip crinkle virus also increased SA levels in cuticle waxes (fig. S5B). These results suggested that increased SA accumulation in cuticle wax may not be pathogen specific. The ssi2 mutant, which is constitutively activated in pathogen defense and contains high basal SA (40), also contained more SA in cuticle wax than wild-type plants (fig. S5C, left). Likewise, transient overexpression of SID2 in Nicotiana benthamiana increased SA levels in cuticle wax (fig. S5C, right). SA was detected in the cuticle wax of numerous healthy plants including tomato, sweet potato, potato, zucchini, and pea (Fig. 6D). In contrast, BA, which was also detected in cuticle wax, did not accumulate in response to pathogen infection or the ssi2 mutation (fig. S5D). Most of the SA present in waxes was derived from the SID2-catalyzed reaction, since the sid2 mutant contained significantly reduced levels of basal and pathogen-responsive SA (fig. S5E).

Analysis of acp4 and mod1 plants showed that both contained significantly higher than wild-type levels of basal and pathogeninducible SA in their cuticle wax (Fig. 6E). This supported the notion that increased transpiration due to high cuticle permeability promoted SA efflux into cuticle wax and in turn reduced apoplastic SA in these mutants. To test this possibility, we first quantified wax SA levels in Col-0 and *mod1* plants grown at 65 or 90% relative humidity. The mod1 plants showed a significant reduction in their basal wax SA levels (fig. S6A), suggesting that export of SA into cuticle wax was likely regulated by transpiration. These results further suggest that transpirational pull may also be responsible for directing SA toward the plasma membrane. If this were true, less cytosolic SA would be available for defense signaling in cuticle defective mutants. Both PR-1 transcript and PR-5 protein were induced to a lesser extent in acp4 and mod1 plants at early time point (18 hours) after pathogen infection but accumulated at wild-type-like levels by 48 hours when SA accumulation was maximum (Figs. 1A and 6, F and G). These results further suggested that SA may be first directed outward to the apoplast before it begins accumulating in the cytoplasm. This is supported by the fact that the eds1-1 and pad4-1 mutants, which accumulate significantly reduced leaf SA (41), contain wild-type-like levels of SA in PEX after pathogen infection (fig. S6, B and C). Likewise, a significant portion of SA is transported to PEX in nahG plants, even though they contain very low levels of SA (Fig. 4, B and C, and fig. S3B). Together, these results support the notion that transport of SA into apoplast precedes its accumulation into cytosol.

SA and water potential regulates stomatal opening

To determine the biological relevance of SA in cuticle wax, we first compared the wax profiles of wild-type and sid2 plants after SA application. SA did not alter the total wax content or wax profile of wild-type or sid2 plants (Fig. 7, A and B). Furthermore, reduced wax SA did not alter the cuticle permeability of sid2 plants (fig. S7A), indicating that SA did not affect cuticle wax or permeability. Notably, however, sid2 plants did show increased stomatal aperture, reduced water potential, and reduced WUE (Fig. 7, C to F). Furthermore, exogenous SA, but not pathogen infection, restored stomatal aperture

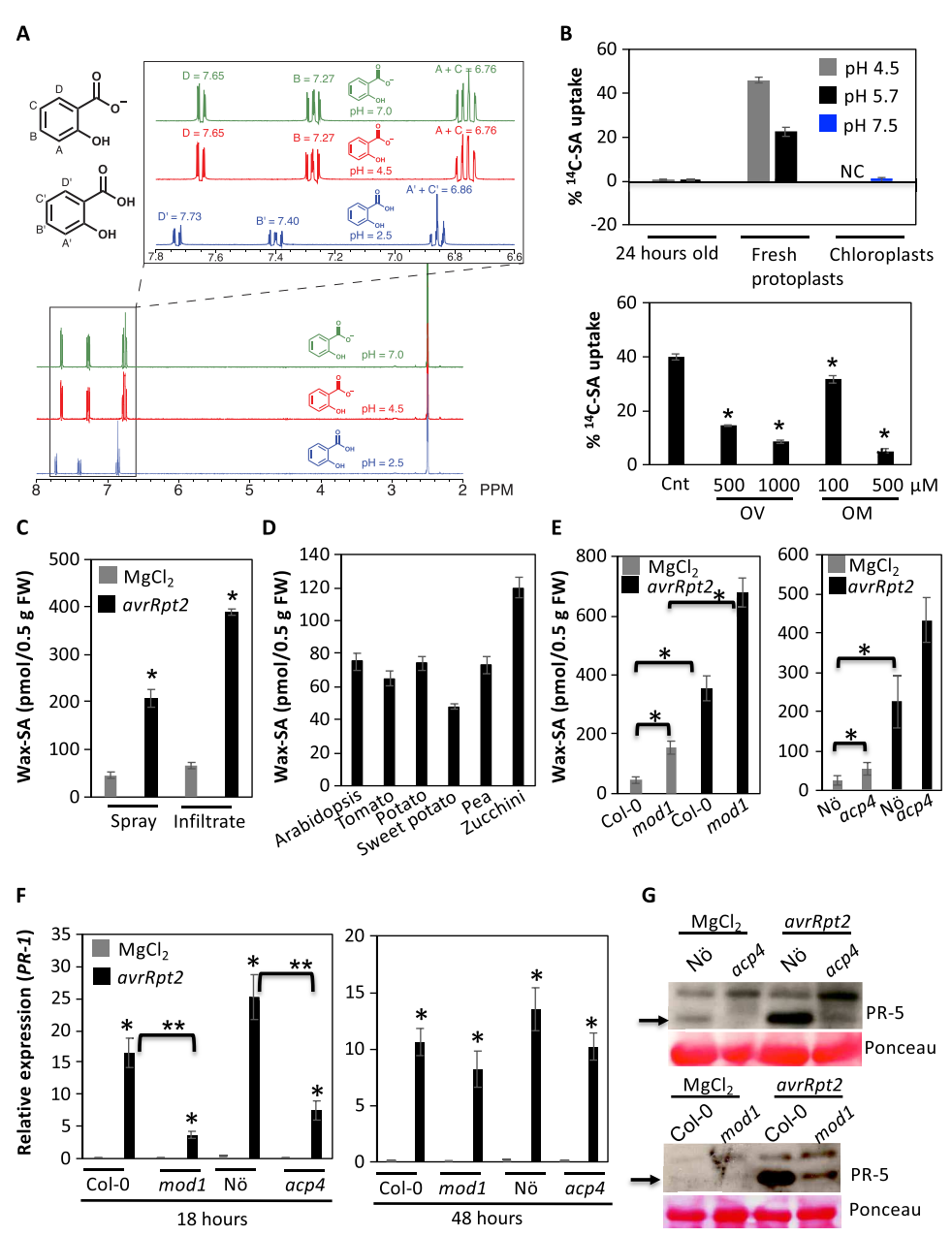


Fig. 6. SA exists in a deprotonated form at cytosolic pH and is exported into cuticular waxes. (**A**) NMR spectra of SA at pH 2.5, 4.5, and 7.0. The samples were made in DMSO-d₆ containing 400 μl of buffered solution of SA. The transmitter offset frequency was placed at the corresponding water peak (4.506 ppm for pH 2.5 and 4.5 and 4.513 ppm for pH 7). All samples were then referenced to DMSO (2.5 ppm). (**B**) Top: Uptake assays showing percentage of ¹⁴C-SA transported into isolated protoplasts or chloroplasts. Fresh or 24-hour-old protoplasts (10^6 /ml) or chloroplast (10^7 /ml) were incubated with 2 μM ¹⁴C-SA for 1 hour, analyzed microscopically before and after four washes, and quantified for the amount of radiolabel. NC indicates data not considered since chloroplasts were damaged after 1-hour incubation at pH 4.5. The experiment was repeated three times with similar results. Bottom: Uptake assays showing percentage of ¹⁴C-SA transported into isolated protoplasts in the absence (control; Cnt) or presence of proton pump inhibitors sodium orthovanadate (OV) and omeprazole (OM). The experiment was repeated two times with similar results. (**C**) SA levels in cuticular wax fraction of mock- and *avrRpt2*-inoculated leaves. Leaves were sprayed (10^8 CFU/ml) or infiltrated (10^5 CFU/ml) with *avrRpt2* and sampled 48 hours after inoculation. (**D**) Relative SA levels in cuticular wax fraction of indicated plants. The experiment was repeated three times with similar results. (**E**) SA levels in cuticular wax fraction of mock- and *avrRpt2*-inoculated leaves. Leaves were sprayed (10^8 CFU/ml) with *avrRpt2* and sampled 48 hours after inoculation. Asterisks denote a significant difference (t test, P < 0.0015). (**F**) Real-time quantitative RT-PCR showing relative expression levels of *PR-1* in mock- and *avrRpt2*-inoculated plants at 18 and 48 hours after inoculation. The error bars indicate SD (n = 3). Results are representative of two independent experiments. Single and double asterisks denote a si

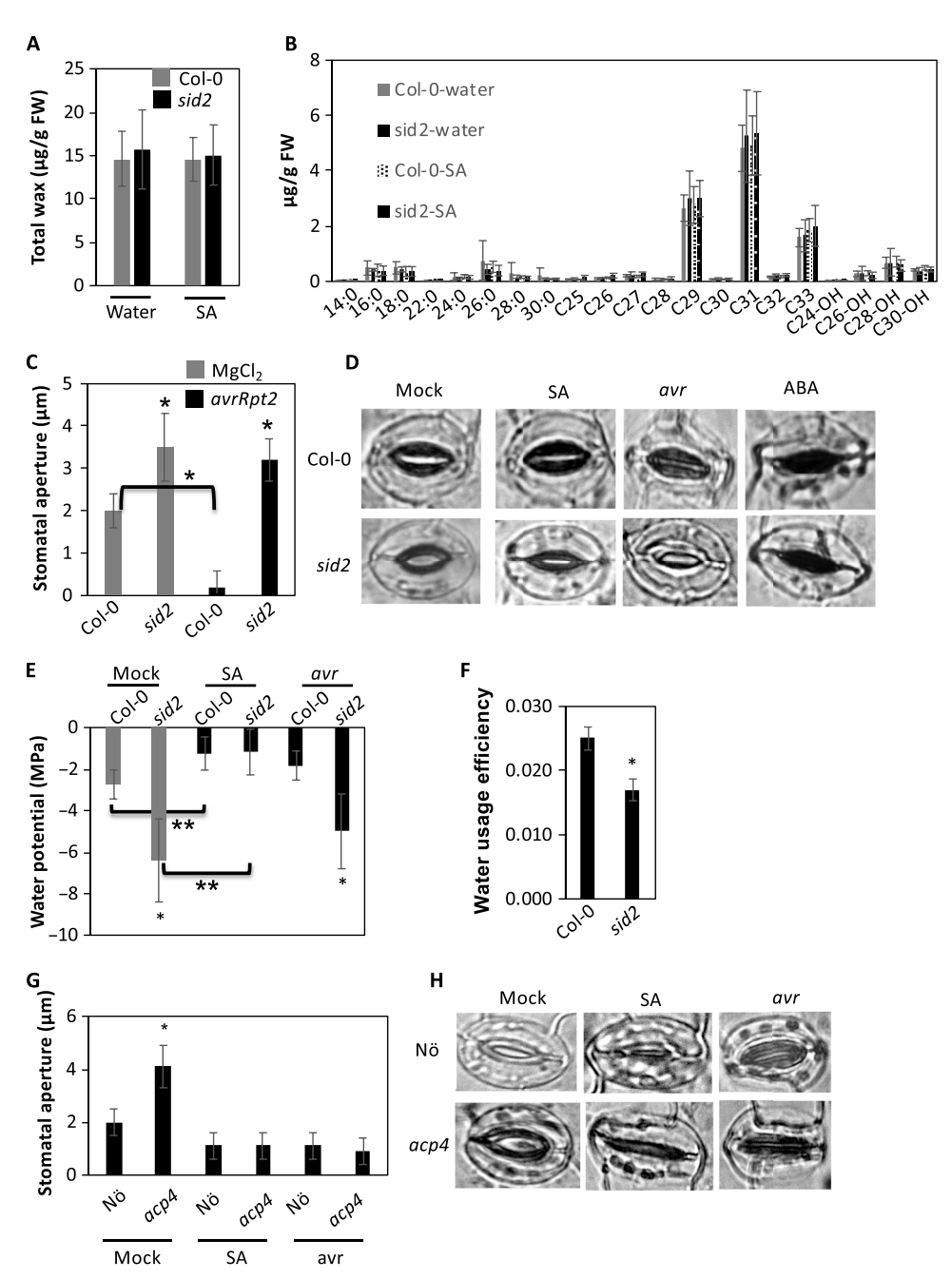


Fig. 7. Cuticular SA regulates stomatal opening. (**A**) Total wax levels in Col-0 and *sid2* plants treated with water or 500 μM SA for 24 hours before wax extraction. The experiment was repeated two times with similar results. (**B**) Analysis of wax components from leaves of 4-week-old Col-0 and *sid2* plants that were treated with water or 500 μM SA for 24 hours before wax extraction. 16:0 to 24:0 are FAs, C25 to C33 are alkanes, and C26-OH to C30-OH are primary alcohols. The experiment was repeated two times with similar results. (**C**) Stomatal apertures in mock- and *avrRpt2*-inoculated leaves of Col-0 and *sid2* plants 24 hours after infection. Values are means \pm SD (n = 20). Single and double asterisks denote a significant difference between Col-0 and *sid2* and between indicated pairs, respectively (t test, t < 0.003). (**D**) Microscopic images showing representative stomata of mock-, pathogen (t = 24 hours. Values are means t = 25 (t = 15). Single and double asterisks denote a significant difference between Col-0 and *sid2* and between indicated pairs, respectively (t test, t < 0.0001). (**F**) WUE for Col-0 and *sid2* plants. Values are means t = 20 (t = 4). Asterisks denote a significant difference (t test, t < 0.005). (**G**) Stomatal apertures in mock-, t = 20.001). (**F**) WUE for Col-0 and t = 20 (t = 20). Asterisks denote a significant difference (t test, t < 0.0001). (**H**) Microscopic images showing representative stomata of mock-, SA (500 μM)-, or t = 20. Asterisks denote a significant difference (t test, t < 0.0001). (**H**) Microscopic images showing representative stomata of mock-, SA (500 μM)-, or t = 20. Asterisks denote a significant difference (t test, t < 0.0001). (**H**) Microscopic images showing representative stomata of mock-, SA (500 μM)-, or t = 20. Asterisks denote a significant difference (t test, t < 0.0001). (**H**) Microscopic images showing representative stomata of mock-, SA (500 μM)-, or t = 20.0001.

and water potential in these plants (Fig. 7, D and E). This was consistent with the result that a significant portion of exogenously applied SA was retained in the cuticle wax of wild-type plants (fig. S7B). Like SA, exogenous treatment with ABA induced stomatal closure in *sid2*

plants (Fig. 7D). However, SA-induced stomatal closure was likely independent of ABA because SA treatment did not induce JA or ABA levels (data not shown) or expression of JA- or ABA-responsive genes in Col-0 plants (fig. S7C) (42). On the other hand, both SA and pathogen

infection resulted in reduced stomatal aperture of *acp4* plants (Fig. 7, G and H). Exogenous SA also reduced stomatal aperture in *mod1* plants (fig. S7D). Together, these results suggest that the relative water and SA content in the epidermis regulate stomatal closure; increased flux of SA into cuticle wax promotes stomatal closure after pathogen infection, a mechanism that may have evolved to prevent further pathogen entry through these openings.

DISCUSSION

Here, we report major findings related to the transport of SA during SAR and the involvement of the plant cuticle in this process. We show that SA transported out of the chloroplast is routed to the cell exterior (fig. S8) and the cuticle. We further show that the transpirational pull and water potential inside the cell regulate transport of SA through the apoplast. Consequently, cuticle impaired mutants, which exhibit increased transpiration, contain relatively more SA in cuticle wax. Three different mutants, altered in either wax (mod1) or cutin (lacs2) (27, 28) alone, or altered in both wax and cutin (acp4) (3) content, were examined, and all showed impaired SA transport. This supports the conclusion that cuticle permeability, rather than specific defects in wax or cutin biosynthesis, regulates SA transport. Although movement of SA into cuticle wax is expected to involve transport via the apoplast, the cuticle mutants acp4 and mod1 accumulated low levels of SA in their apoplast. This suggests that the transpirational force in acp4 and mod1 likely exceeds horizontal apoplastic transport and forces most of SA out of apoplast into cuticular waxes. It is possible that once transported outside, SA may be retained in the cuticle possibly due to the outward transpirational pull.

Despite its structural similarity to SA (fig. S9), BA is not transported in a transpiration- or water potential—dependent manner because *acp4* and *mod1* plants contain wild-type levels of BA in apoplast and cuticle. This suggests that any potential plasma membrane—associated SA transporter is specific to SA. SA has a lower pKa than BA, and, unlike in BA, an internal hydrogen bond in SA delocalizes the negative charge and increases its membrane permeability (fig. S9)(43). Thus, it is possible that the structural properties of SA together with pH differential between apoplast and symplast and overall water potential are important driving forces responsible for SA transport.

A recent study has shown that SA biosynthesis takes place in the cytosol (fig. S8) (44). As SA accumulates in response to pathogen infection, H⁺ levels in the cytosol are expected to rise due to deprotonation of the accumulating SA. This increase in H⁺ is likely to result in a proton differential across the plasma membrane, thereby facilitating transport of SA into the apoplast. Unlike the chloroplast membrane, SA is able to permeate the plasma membrane bidirectionally, and this is consistent with the initial transport of SA to the apoplast in infected leaves followed by subsequent reentry into the symplast of distal uninfected cells (fig. S8). In animals, monocarboxylate transporters, which catalyze proton-linked transport of specific monocarboxylates, facilitate SA transport across animal plasma membranes (45). Aspirin, the wellknown pharmaceutical derivative of SA, is thought to be transported in a pH- and carrier protein-dependent manner (45, 46). A similar scenario has also been suggested for Ricinus (47) and supported by our results. Whether protonated and unprotonated species of SA exist in an equilibrium and if that governs transport of SA remain unknown

The cuticle defect in *acp4* and *mod1* plants does not affect PD gating and, thereby, G3P transported through the symplast. Thus, the SAR

defect of acp4 and mod1 plants can be attributed to their inability to transport SA systemically. This is supported by the fact that acp4 and mod1 plants contain reduced Pip in distal, uninfected tissue. Furthermore, locally applied exogenous SA cannot induce SAR in acp4 and mod1 plants. This correlates with the fact that SA accumulation in distal tissue is important for distal Pip accumulation and, thereby, onset of SAR. However, this is contrary to the current consensus that transport of SA from local to distal tissues is not required for SAR. This assumption was primarily based on the finding that grafts between wild-type rootstock and nahG scions were SAR compromised, whereas the reciprocal graft was SAR competent (10). The study concluded that although presence of SA in distal tissue is essential for SAR, its transport from infected to distal leaves is not. One possibility, as suggested by Vernooij et al. (10), is that an additional, as yet unknown, signal is transported to distal tissue, where it induces de novo synthesis of SA. However, both *acp4* and *mod1* clearly generate this potential unknown signal because PEX from acp4 or mod1 plants can induce SAR on wild-type plants. Yet, pathogen infection is unable to induce wild-type-like PR-5 accumulation in the distal tissue of these plants, contradicting the possibility of an unknown transported signal inducing distal de novo SA synthesis. On the basis of our results, we propose that accumulation of SA at threshold levels is essential for induction of SAR in the distal leaves. SA transported from the wild-type rootstock is converted to catechol in the nahG scion and is therefore unavailable to reinitiate the SA/G3P-Pip feedback loop (16). On the other hand, SA transported from nahG rootstock to wild-type scion can initiate signaling, which is sustained due to the SA biosynthetic competency of the wild-type scion, resulting in SAR. These results support the crucial role of SA as an essential mobile signal in SAR.

MATERIALS AND METHODS

Plant growth conditions and genetic analysis

Plants were grown in MTPS 144 Conviron (Winnipeg, MB, Canada) walk-in chambers at 22°C, 65% relative humidity, and 14-hour light and 10-hour dark photoperiod. These chambers were equipped with cool white fluorescent bulbs (Sylvania, FO96/841/XP/ECO). The photon flux density of the day period was 106.9 μ mol m⁻² s⁻¹ (measured using a digital light meter, Phytotronic Inc., MO). Plants were grown on autoclaved Pro-Mix soil (Premier Horticulture Inc., PA, USA). Soil was fertilized once using Scotts Peter's 20:10:20 peat lite special general fertilizer that contained 8.1% ammoniacal nitrogen and 11.9% nitrate nitrogen (Scottspro.com). Plants were irrigated using deionized or tap water. The *acp4* and *mod1* plants used in this study are described earlier (3, 22).

Grafting between wild-type (N background) and nahG (N background) plants was carried out at the vegetative stage. A vertical slit was made in the root stalk, above the third leaf from the base, and grafted with a wedge-shaped shoot with two to three newly developing leaves. Grafts were secured in place by wrapping the graft junction with parafilm. Plants were kept in a transparent box covered with saran wrap for 3 to 4 days and inoculated with TMV 10 days after grafting.

RNA extraction, quantitative real-time polymerase chain reaction

Small-scale extraction of RNA from two or three leaves (per sample) was performed with the TRIzol reagent (Invitrogen, CA) following the manufacturer's instructions. RNA quality and concentration were

determined by gel electrophoresis and determination of A_{260} (absorbance at 260 nm). Reverse transcription (RT) and first-strand cDNA (complementary DNA) synthesis were carried out using Superscript II (Invitrogen, CA). Quantitative RT polymerase chain reaction (RT-PCR) was carried out as described before (48). Each sample was run in triplicates, and ACTINII (At3g18780) expression levels were used as internal control for normalization. Cycle threshold values were calculated by SDS 2.3 software.

Protein extraction and immunoblot analysis

Proteins were extracted in buffer containing 50 mM tris-HCl (pH7.5), 10% glycerol, 150 mM NaCl, 10 mM MgCl₂, 5 mM EDTA, 5 mM dithiothreitol, and 1× protease inhibitor cocktail (Sigma-Aldrich, St. Louis, MO). Protein concentration was measured by the Bio-Rad protein assay (Bio-Rad, CA). For Ponceau-S staining, polyvinylidene difluoride (PVDF) membranes were incubated in Ponceau-S solution [40% methanol (v/v), 15% acetic acid (v/v), and 0.25% Ponceau-S]. The membranes were destained using deionized water. Proteins (~50 µg) were fractionated on a 7 to 10% SDS-polyacrylamide gel electrophoresis and subjected to immunoblot analysis using ∞ -PR-1 (tobacco) or ∞ -PR-5 (*Arabidopsis*) antibodies (Agrisera). Immunoblots were developed using ECL (enhanced chemiluminesence) detection kit (Roche) or alkaline phosphatase–based color detection.

Pathogen infection and collection of phloem exudate and apoplastic fluid

Inoculations with *Pseudomonas syringae* DC3000 were conducted as described before (3). The bacterial cultures were grown overnight in King's B medium containing rifampicin and/or kanamycin. For analysis of SAR, the primary leaves were inoculated with MgCl₂ or the *avr* bacteria (10⁶ cfu ml⁻¹), and 24 hours later, the systemic leaves were inoculated with *vir* bacteria (10⁵ cfu ml⁻¹). Unless noted otherwise, samples from the systemic leaves were harvested at 3 dpi. Petiole exudates were collected as described earlier (12, 14). PEX was assayed for bacterial growth to ensure that it did not contain any viable bacteria. Apoplastic fluid was collected as described earlier (49). The purity of apoplastic fluid was assayed by quantifying Pip levels, which is not present in the apoplastic fluid.

Chemical treatments

SA, G3P, AzA, Pip, and ABA treatments were carried out by using 500, 100, 1000, 1000, and 100 μM solutions, respectively. AzA was prepared in methanol and diluted in water. SA, G3P, and Pip were prepared and diluted in water. Sodium orthovanadate and omeprazole stocks were prepared in water or dimethyl sulfoxide (DMSO), respectively, and the working concentration was prepared in protoplast buffer. All dilutions were freshly prepared before performing biological experiments.

G3P, SA, Pip, JA, and ABA quantifications

G3P quantifications were carried out as described earlier (12). SA and SAG were extracted and measured from ~ 0.1 g of FW leaf tissue, as described before (50). Pip quantifications were carried out using gas chromatography (GC)–MS (16). For quantification of SA and BA levels in wax extracts, the chloroform extracts were dried under a gentle stream of nitrogen gas, and samples were derivatized with N-methyl-N-(tert-butyldimethylsilyl) trifluoroacetamide (MTBSTFA) containing 1% tert-butyldimethylchlorosilane (TBDMCS) and analyzed by GC-MS. JA and ABA were extracted from ~ 0.5 g of FW leaf tissue. The leaf

tissue was ground in liquid nitrogen with 100 ng of heptadecanoic acid (17:0) (Sigma-Aldrich) and extracted into 7 ml of methanol, dried under a gentle stream of nitrogen gas, resuspended in 1% acetic acid, and loaded onto a 500-mg C18 reverse-phase Sep-Pak column prewashed with 5 volumes of methanol followed by 5 volumes of 1 M acetic acid. The column was then washed with 5 volumes of 1 M acetic acid, and the sample was eluted with 5 volumes of methanol. The sample was dried under a stream of nitrogen, derivatized with diazomethane, and analyzed by GC-MS using selected ion-monitoring mode.

FA and lipid analysis

FA extraction was carried out by placing leaf tissue in 2 ml of 3% $\rm H_2SO_4$ in methanol. After 30 min of incubation at 80°C, 1 ml of hexane with 0.001% butylated hydroxytoluene (BHT) was added. The hexane phase was then transferred to vials for GC analysis. One-microliter samples were analyzed by GC on a Varian FAME 0.25 mm by 50 m column and quantified with flame ionization detection. For quantification of FAs, leaves (50 mg) were extracted together with an internal standard 17:0 (Sigma-Aldrich), and the FA levels were calculated on the basis of the detected peak areas corresponding to the FA retention time relative to the areas of the internal standard.

For lipid extraction, six to eight leaves were incubated at 75° C in isopropanol containing 0.001% BHT for ~15 min. To this, 1.5 ml of chloroform and 0.6 ml of water were added, and the samples were agitated at room temperature for 1 hour. The lipids were reextracted in chloroform: methanol (2:1) until the leaves were bleached. The aqueous content was removed by partitioning with 1 M KCl and water. The lipid extract was dried under a gentle stream of nitrogen gas and redissolved in 0.5 ml of chloroform. Lipid analysis and acyl group identification were carried out using the automated electrospray ionization–tandem MS facility at Kansas Lipidomics Research Center.

Analysis of wax and cutin components

For analysis of the wax components, 500 mg of 4-week-old leaves was immersed in 10 ml of chloroform for 10 s. The leaves were rinsed once more with 10 ml of chloroform for 10 s. An internal standard (20 μ g of n-tetracosane) was added, and the extract was evaporated under a gentle stream of nitrogen. The samples were derivatized using diazomethane followed by 100 μ l of pyridine and 100 μ l of acetic anhydride. The sealed tubes were incubated for 1 hour at 60°C. The samples were again dried under a gentle stream of nitrogen and dissolved in 0.5 ml of heptane:toluene (1:1, v/v). The solution was washed with 400 μ l of 1% NaHCO₃ before GC-MS analysis.

Cutin monomer composition and content were determined using the sodium methoxide–catalyzed transmethylation method followed by acetylation of the hydroxyl groups, with acetic anhydride and GC-MS slightly modified as previously described (1, 51). After methanolysis, the methylene dichloride extract of cutin monomers was washed with 0.9% potassium chloride instead of 0.5 M sodium chloride. Both wax and cutin extracts were analyzed using GC-MS analysis on an HP-5 capillary column.

SA transport assays

For SA transport, [14 C] SA (1 μ Ci/ml; specific activity, 50 mCi/mmol; PerkinElmer Inc.) was suspended in 10 mM MgCl₂ and used for infiltrations with or without *avrRpt2*. The resulting solution contained 20 μ M SA and was injected into the abaxial surface of 4-week-old *Arabidopsis* leaves. Three leaves per plant were infiltrated with ~0.05 ml of 14 C-SA solution. The plants were then kept in a growth

chamber set at 14-hour light and 10-hour dark photoperiods. The leaf samples were extracted using the SA extraction method described before (50). The samples were quantified using a liquid scintillation counter, and extracts containing [¹⁴C] radioactivity were loaded onto a silica gel 60 thin-layer chromatography (TLC) plate and developed using toluene: methanol: acetic acid (45:8:4, by volume). The TLC plates were exposed in a storage phosphorimage screen (GE), and the bands were visualized by Typhoon PhosphorImager.

Measuring plasmodesmal permeability

Intact leaves of 3-week-old soil-grown *Arabidopsis* plants were bombarded with a plasmid for expression of GFP using microprojectile bombardment as previously described (*52*). Three biological replicates in duplicate were performed. Bombarded plants were kept in growth chambers for 24 hours before individual transformed cells were identified using a Leica SP8 White Light Laser confocal microscope using the 488-nm line of the argon ion laser for excitation and emission collected between 505 and 530 nm. Layers of cells containing trafficked GFP surrounding the transformed cells were counted. Images were collected with a 25× 0.95 NA water immersion lens.

Protoplast and chloroplast transport assays

Chloroplasts and protoplasts were prepared as described before (53, 54), quantified using a hemocytometer, and suspended at a concentration of $10^7/\text{ml}$ or $10^6/\text{ml}$, respectively. For transport assays, 50 to $100~\mu l$ of chloroplasts or protoplasts was incubated with 2 μM $^{14}\text{C-SA}$ for 1 hour, analyzed microscopically before and after four washes, and quantified for the amount of radiolabel using a liquid scintillation counter.

Water use efficiency and water potential

To test for WUE, we measured gas exchange (in light; $500 \,\mu\text{mol m}^{-2}\,\text{s}^{-1}$) of an open-flow system (LI-6800, Li-Cor, Lincoln, Nebraska, USA) equipped with a multiphase flash fluorometer as the light source. In the sample chamber, air temperature was set to 24°C, relative humidity at 70%, airflow rate at 500 μmol s⁻¹, and the sample CO₂ at 400 µmol mol⁻¹. Leaves that were still attached to the plants were placed in the 6-cm² area chamber, and because the leaves were smaller than 6 cm², normalization of WUEs was carried out. The infrared gas analyzers (sample and reference) were matched before assays of each leaf. After gas exchange equilibrated, for each leaf and at each light level, three measures were logged. These three measures were used to estimate the mean photosynthetic condition of the leaf, and this mean was used in the analysis. WUE is calculated as the assimilation and transpiration rate. Water potential was quantified using a pressure chamber (model 3000, Soilmoisture Equipment Corp., Santa Barbara, CA USA).

Nuclear magnetic resonance

NMR spectra of SA at varying pH were collected using a 400-MHz Bruker Avance NEO NMR (Billerica, MA, USA). The samples were made with 300 μ l of DMSO-d₆ and 400 μ l of sample in buffer solution of corresponding pH 2.5, 4.5, or 7.0. The pulse sequence used for NMR analysis was a Bruker standard sequence "zgesgp," which is a water suppression sequence using excitation sculpting with gradients. The transmitter offset frequency was placed at the corresponding water peak (4.506 ppm for pH 2.5 and 4.5, 4.513 ppm for pH 7). All samples were then reference to DMSO (2.5 ppm). Assignments made via comparison of assignments as described before (55).

Statistics and reproducibility

For pathogen assays, ~16 plants/genotype/treatment were analyzed in a single experiment. At least three to four technical replicates/genotype/treatment were plated. For metabolite quantification, ~12 plants/genotype/treatment were analyzed in each experiment. Experiments were repeated at least two to three times with a different set of plants as indicated in the figure legends. Unless otherwise mentioned, error bars indicate SD.

SUPPLEMENTARY MATERIALS

Supplementary material for this article is available at http://advances.sciencemag.org/cgi/content/full/6/19/eaaz0478/DC1

View/request a protocol for this paper from Bio-protocol.

REFERENCES AND NOTES

- I. Molina, G. Bonaventure, J. Ohlrogge, M. Pollard, The lipid polyester composition of Arabidopsis thaliana and Brassica napus seeds. Phytochemistry 67, 2597–2610 (2006).
- G.-H. Lim, R. Singhal, A. Kachroo, P. Kachroo, Fatty acid and lipid-mediated signaling in plant defense. *Annu. Rev. Phytopathol.* 55, 505–536 (2017).
- Y. Xia, Q.-M. Gao, K. Yu, L. Lapchyk, D. R. Navarre, D. Hildebrand, A. Kachroo, P. Kachroo, An intact cuticle in distal tissues is essential for the induction of systemic acquired resistance in plants. *Cell Host Microbe* 5, 151–165 (2009).
- Y. Xia, K. Yu, Q.-M. Gao, E. V. Wilson, D. Navarre, P. Kachroo, A. Kachroo, Acyl CoA binding proteins are required for cuticle formation and plant responses to microbes. *Front. Plant Sci.* 3, 224 (2012).
- Y. Xia, K. Yu, D. Navarre, K. Seebold, A. Kachroo, P. Kachroo, The glabra1 mutation affects cuticle formation and plant responses to microbes. Plant Physiol. 154, 833–846 (2010).
- D. Wendehenne, Q.-m. Gao, A. Kachroo, P. Kachroo, Free radical-mediated systemic immunity in plants. Curr. Opin. Plant Biol. 20, 127–134 (2014).
- A. Singh, G.-H. Lim, P. Kachroo, Transport of chemical signals in systemic acquired resistance. J. Integr. Plant Biol. 59, 336–344 (2017).
- M. B. Shine, X. Xiao, P. Kachroo, A. Kachroo, Signaling mechanisms underlying systemic acquired resistance to microbial pathogens. *Plant Sci.* 279, 81–86 (2019).
- T. Gaffney, L. Friedrich, B. Vernooij, D. Negrotto, G. Nye, S. Uknes, E. Ward, H. Kessmann, J. Ryals, Requirement of salicylic acid for the induction of systemic acquired resistance. Science 261, 754–756 (1993).
- B. Vernooij, L. Friedrich, A. Morse, R. Reist, R. Kolditz-Jawhar, E. Ward, S. Uknes, H. Kessmann, J. Ryals, Salicylic acid is not the translocated signal responsible for inducing systemic acquired resistance but is required in signal transduction. *Plant Cell* 6, 959–965 (1994).
- G.-H. Lim, M. B. Shine, L. de Lorenzo, K. Yu, W. Cui, D. Navarre, A. G. Hunt, J.-Y. Lee, A. Kachroo, P. Kachroo, Plasmodesmata localizing proteins regulate transport and signaling during systemic acquired immunity in plants. *Cell Host Microbe* 19, 541–549 (2016).
- B. Chanda, Y. Xia, M. K. Mandal, K. Yu, K.-T. Sekine, Q.-m. Gao, D. Selote, Y. Hu,
 A. Stromberg, D. Navarre, A. Kachroo, P. Kachroo, Glycerol-3-phosphate is a critical mobile inducer of systemic immunity in plants. *Nat. Genet.* 43, 421–427 (2011).
- Q.-m. Gao, K. Yu, Y. Xia, M. B. Shine, C. Wang, D. Navarre, A. Kachroo, P. Kachroo, Mono- and digalactosyldiacylglycerol lipids function nonredundantly to regulate systemic acquired resistance in plants. *Cell Rep.* 9, 1681–1691 (2014).
- C. Wang, M. El-Shetehy, M. B. Shine, K. Yu, D. Navarre, D. Wendehenne, A. Kachroo, P. Kachroo, Free radicals mediate systemic acquired resistance. *Cell Rep.* 7, 348–355 (2014).
- K. Yu, J. M. Soares, M. K. Mandal, C. Wang, B. Chanda, A. N. Gifford, J. S. Fowler, D. Navarre, A. Kachroo, P. Kachroo, A feedback regulatory loop between G3P and lipid transfer proteins DIR1 and AZI1 mediates azelaic-acid-induced systemic immunity. *Cell Rep.* 3, 1266–1278 (2013).
- C. Wang, R. Liu, G.-H. Lim, L. de Lorenzo, K. Yu, K. Zhang, A. G. Hunt, A. Kachroo,
 P. Kachroo, Pipecolic acid confers systemic immunity by regulating free radicals. Sci. Adv.
 4. eaar4509 (2018).
- D. Wendehenne, J. Durner, D. F. Klessig, Nitric oxide: A new player in plant signalling and defence responses. Curr. Opin. Plant Biol. 7, 449–455 (2004).
- H. Návarová, F. Bernsdorff, A.-C. Doring, J. Zeier, Pipecolic acid, an endogenous mediator of defense amplification and priming, is a critical regulator of inducible plant immunity. Plant Cell 24, 5123–5141 (2012).
- M. Hartmann, T. Zeier, F. Bernsdorff, V. Reichel-Deland, D. Kim, M. Hohmann, N. Scholten, S. Schuck, A. Bräutigam, T. Hölzel, C. Ganter, J. Zeier, Flavin monooxygenase-generated N-hydroxypipecolic acid is a critical element of plant systemic immunity. *Cell* 173, 456–469.e16 (2018).

SCIENCE ADVANCES | RESEARCH ARTICLE

- Y. C. Chen, E. C. Holmes, J. Rajniak, J. G. Kim, S. Tang, C. R. Fischer, M. B. Mudgett, E. S. Sattely, N-hydroxy-pipecolic acid is a mobile metabolite that induces systemic disease resistance in Arabidopsis. Proc. Natl. Acad. Sci. U.S.A. 115, E4920–E4929 (2018).
- 21. P. Kachroo, A. Kachroo, Plants pack a quiver full of arrows. *Cell Host Microbe* 23, 573–575
- Z. Mou, Y. He, Y. Dai, X. Liu, J. Li, Deficiency in fatty Acid synthase leads to premature cell death and dramatic alterations in plant morphology. *Plant Cell* 12, 405–418 (2000).
- M. C. Wildermuth, J. Dewdney, W. Gang, F. M. Ausubel, Isochorismate synthase is required to synthesize salicylic acid for plant defence. *Nature* 414, 562–565 (2001).
- W. Molders, A. Buchala, J.-P. Metraux, Transport of salicylic acid in tobacco necrosis virus-infected cucumber plants. *Plant Physiol.* 112, 787–792 (1996).
- T. Tanaka, H. Tanaka, C. Machida, M. Watanabe, Y. Machida, A new method for rapid visualization of defects in leaf cuticle reveals five intrinsic patterns of surface defects in *Arabidopsis*. *Plant J.* 37, 139–146 (2004).
- S. Kurdyukov, A. Faust, C. Nawrath, S. Bär, D. Voisin, N. Efremova, R. Franke, L. Schreiber, H. Saedler, J.-P. Métraux, A. Yephremov, The epidermis-specific extracellular BODYGUARD controls cuticle development and morphogenesis in *Arabidopsis. Plant Cell* 18. 321–339 (2006).
- J. Schnurr, J. Shockey, J. Browse, The acyl-CoA synthetase encoded by LACS2 is essential for normal cuticle development in Arabidopsis. Plant Cell 16, 629–642 (2004).
- M. Bessire, C. Chassot, A. C. Jacquat, M. Humphry, S. Borel, J. M. Petétot, J. P. Métraux, C. Nawrath, A permeable cuticle in *Arabidopsis* leads to a strong resistance to *Botrytis cinerea*. *EMBO J.* 26. 2158–2168 (2007).
- L. Liu, F.-M. Sonbol, B. Huot, Y. Gu, J. Withers, M. Mwimba, J. Yao, S. Y. He, X. Dong, Salicylic acid receptors activate jasmonic acid signalling through a non-canonical pathway to promote effector-triggered immunity. *Nat. Commun.* 7, 13099 (2016).
- K. Gruner, T. Griebel, H. Návarová, E. Attaran, J. Zeier, Reprogramming of plants during systemic acquired resistance. Front. Plant Sci. 4, 252 (2013).
- L. A. J. Mur, Y.-M. Bi, R. M. Darby, S. Firek, J. Draper, Compromising early salicylic acid accumulation delays the hypersensitive response and increases viral dispersal during lesion establishment in TMV-infected tobacco. *Plant J.* 12, 1113–1126 (1997).
- S. M. Assmann, J. A. Snyder, Y. R. J. Lee, ABA-deficient (aba1) and ABA-insensitive (abi1-1, abi2-1) mutants of *Arabidopsis* have a wild-type stomatal response to humidity. *Plant Cell Environ.* 23, 387–395 (2000).
- R. Morillon, M. J. Chrispeels, The role of ABA and the transpiration stream in the regulation of the osmotic water permeability of leaf cells. Proc. Natl. Acad. Sci. U.S.A. 98, 14138–14143 (2001)
- M. Yasuda, A. Ishikawa, Y. Jikumaru, M. Seki, T. Umezawa, T. Asami, A. Maruyama-Nakashita, T. Kudo, K. Shinozaki, S. Yoshida, H. Nakashita, Antagonistic interaction between systemic acquired resistance and the abscisic acid–mediated abiotic stress response in *Arabidopsis*. *Plant Cell* 20, 1678–1692 (2008).
- S. Panchal, R. Chitrakar, B. K. Thompson, N. Obulareddy, D. Roy, W. S. Hambright, M. Melotto, Regulation of stomatal defense by air relative humidity. *Plant Physiol.* 172, 2021–2032 (2016).
- A. J. Libbey Jr., J. T. Stock, Dissociation constants of sulfamic acid, salicylic acid, thymol blue, and bromocresol green in anhydrous N,N-dimethylformamide. Anal. Chem. 42, 526–529 (1970)
- T. N. Bibikova, T. Jacob, I. Dahse, S. Gilroy, Localized changes in apoplastic and cytoplasmic pH are associated with root hair development in *Arabidopsis thaliana*. *Development* 125, 2925–2934 (1998).
- B. J. Bowman, C. W. Slayman, The effects of vanadate on the plasma membrane ATPase of Neurospora crassa. J. Biol. Chem. 254, 2928–2934 (1979).
- P. Lindberg, A. Brändström, B. Wallmark, H. Mattsson, L. Rikner, K.-J. Hoffmann, Omeprazole: The first proton pump inhibitor. *Med. Res. Rev.* 10, 1–54 (1990).
- P. Kachroo, J. Shanklin, J. Shah, E. J. Whittle, D. F. Klessig, A fatty acid desaturase modulates the activation of defense signaling pathways in plants. *Proc. Natl. Acad. Sci. U.S.A.* 98, 9448–9453 (2001).
- S. Zhu, R.-D. Jeong, S. C. Venugopal, L. Lapchyk, D. R. Navarre, A. Kachroo, P. Kachroo, SAG101 forms a ternary complex with EDS1 and PAD4 and is required for resistance signaling against turnip crinkle virus. *PLOS Pathog.* 7, e1002318 (2011).
- M. L. Berens, K. W. Wolinska, S. Spaepen, J. Ziegler, T. Nobori, A. Nair, V. Krüler, T. M. Winkelmüller, Y. Wang, A. Mine, D. Becker, R. Garrido-Oter, P. Schulze-Lefert, K. Tsuda, Balancing trade-offs between biotic and abiotic stress responses through leaf age-dependent variation in stress hormone cross-talk. *Proc. Natl. Acad. Sci. U.S.A.* 116, 2364–2373 (2019).

- J. Gutknecht, Salicylates and proton transport through lipid bilayer membranes: A model for salicylate-induced uncoupling and swelling in mitochondria. J. Membr. Biol. 115, 253–260 (1990).
- D. Rekhter, D. Lüdke, Y. Ding, K. Feussner, K. Zienkiewicz, V. Lipka, M. Wiermer, Y. Zhang, I. Feussner, Isochorismate-derived biosynthesis of the plant stress hormone salicylic acid. *Science* 365, 498–502 (2019).
- 45. A. P. Halestrap, Monocarboxylic acid transport. Compr. Physiol. 3, 1611–1643 (2013).
- M. Takagi, Y. Taki, T. Sakane, T. Nadai, H. Sezaki, N. Oku, S. Yamashita, A new interpretation of salicylic acid transport across the lipid bilayer: Implications of pHdependent but not carrier-mediated absorption from the gastrointestinal tract. *J. Pharmacol. Exp. Ther.* 285, 1175–1180 (1998).
- F. Rocher, J.-F. Chollet, S. Legros, C. Jousse, R. Lemoine, M. Faucher, D. R. Bush,
 J. L. Bonnemain, Salicylic acid transport in *Ricinus communis* involves a pH-dependent carrier system in addition to diffusion. *Plant Physiol.* 150, 2081–2091 (2009).
- D.-X. Zhang, P. Nagabhyru, C. L. Schardl, Regulation of a chemical defense against herbivory produced by symbiotic fungi in grass plants. *Plant Physiol.* 150, 1072–1082 (2009).
- S. R. Madsen, H. H. Nour-Eldin, B. A. Halkier, in Biotechnology of Plant Secondary Metabolism (Springer, 2016), pp. 35–42.
- A. C. Chandra-Shekara, M. Gupte, D. Navarre, S. Raina, R. Raina, D. Klessig, P. Kachroo, Light-dependent hypersensitive response and resistance signaling against Turnip Crinkle Virus in *Arabidopsis. Plant J.* 45, 320–334 (2006).
- G. Bonaventure, F. Beisson, J. Ohlrogge, M. Pollard, Analysis of the aliphatic monomer composition of polyesters associated with *Arabidopsis* epidermis: Occurrence of octadeca-cis-6, cis-9-diene-1,18-dioate as the major component. *Plant J.* 40, 920–930 (2004).
- K. M. Crawford, P. C. Zambryski, Subcellular localization determines the availability of non-targeted proteins to plasmodesmatal transport. *Curr. Biol.* 10, 1032–1040 (2000).
- 53. J. Klinkenberg, Extraction of chloroplast proteins from transiently transformed *Nicotiana* benthamiana leaves. *Bio-protocol* **4**, e1238 (2014).
- H. Karesch, R. Bilang, I. Potrykus, Arabidopsis thaliana: Protocol for plant regeneration from protoplasts. Plant Cell Rep. 9, 575–578 (1991).
- D. S. Wishart, C. Knox, A. C. Guo, R. Eisner, N. Young, B. Gautam, D. D. Hau, N. Psychogios, E. Dong, S. Bouatra, R. Mandal, I. Sinelnikov, J. Xia, L. Jia, J. A. Cruz, E. Lim, C. A. Sobsey, S. Shrivastava, P. Huang, P. Liu, L. Fang, J. Peng, R. Fradette, D. Cheng, D. Tzur, M. Clements, A. Lewis, A. De Souza, A. Zuniga, M. Dawe, Y. Xiong, D. Clive, R. Greiner, A. Nazyrova, R. Shaykhutdinov, L. Li, H. J. Vogel, I. Forsythe, HMDB: A knowledgebase for the human metabolome. *Nucleic Acids Res.* 37, D603–D610 (2009).

Acknowledgments: We thank J. Li for mod1 seeds, D. Klessig for ∝-PR-1 antibody, and R.-D. Jeong for help with transmission electron microscopy. We thank S. Wolf and R. Jetter for advice, J. Johnson for help with analytical analysis, and W. Havens and A. Crume for technical help. Funding: This work was supported by grants from National Science Foundation (MCB#0421914 and IOS#051909), Kentucky Science and Engineering Foundation (#1244), Kentucky Soybean Board (3084113467), and USDA National Institute of Food and Agriculture (Hatch project 1014539). Author contributions: The SAR experiments, metabolite levels, gene expression, and protein levels were analyzed by G.-H.L. K.Y., H.L., R.L., and P.K. The protoplasts transport assays were carried out by H.L. and K.Y. ¹⁴C-SA-based plant transport assays were carried out by K.Y. PD permeability assays were carried out by T.B.-S. Water potential and WUE assays were carried out by N.M., R.L., and P.K. NMR analysis was carried out by J.K.M. with help from K.Y. and H.L. P.K. conceptualized the research. P.K. and A.K. supervised the project and wrote the manuscript with help from all the authors. Competing interests: The authors declare that they have no competing interests. Data and materials availability: All data needed to evaluate the conclusions in the paper are present in the paper and/or the Supplementary Materials. Additional data related to this paper may be requested from the authors.

Submitted 7 August 2019 Accepted 21 February 2020 Published 6 May 2020 10.1126/sciady.aaz0478

Citation: G.-H. Lim, H. Liu, K. Yu, R. Liu, M. B. Shine, J. Fernandez, T. Burch-Smith, J. K. Mobley, N. McLetchie, A. Kachroo, P. Kachroo, The plant cuticle regulates apoplastic transport of salicylic acid during systemic acquired resistance. *Sci. Adv.* **6**, eaaz0478 (2020).



The plant cuticle regulates apoplastic transport of salicylic acid during systemic acquired resistance

Gah-Hyun Lim, Huazhen Liu, Keshun Yu, Ruiying Liu, M. B. Shine, Jessica Fernandez, Tessa Burch-Smith, Justin K. Mobley, Nicholas McLetchie, Aardra Kachroo and Pradeep Kachroo

Sci Adv 6 (19), eaaz0478. DOI: 10.1126/sciadv.aaz0478

ARTICLE TOOLS http://advances.sciencemag.org/content/6/19/eaaz0478

SUPPLEMENTARY MATERIALS http://advances.sciencemag.org/content/suppl/2020/05/04/6.19.eaaz0478.DC1

REFERENCES

This article cites 54 articles, 22 of which you can access for free http://advances.sciencemag.org/content/6/19/eaaz0478#BIBL

PERMISSIONS http://www.sciencemag.org/help/reprints-and-permissions

Use of this article is subject to the Terms of Service